A Frequency Selection Criterion in Spatially Developing Flows

By *Jean-Marc Chomaz,* Patrick Huerre,† and Larry G. Redekopp*

The possible existence of global modes or self-excited linear resonances in spatially developing systems is explored within the framework of the WKBJ approximation. It is shown that the existence and properties of the dominant global mode may be deduced from the variations of the local absolute frequency $\omega_0(X)$ with distance X. The main results are summarized in two theorems: (1) A system with no region of absolute instability does not sustain temporally growing global modes with an $O(1)$ growth rate. (2) If the singularity X_s closest to the real X-axis of the complex function $\omega_0(X)$ is a saddle point, the most unstable global mode has, to leading order in the WKBJ approximation, a complex frequency $\omega_0(X_s)$. Thus, it will be temporally growing only if Im $\omega_0(X_s)$ is positive.

1. Introduction

The concept of global modes in spatially developing systems has been introduced in several earlier studies [1–5] of the Ginzburg-Landau model with varying coefficients. In the present context, a global mode is a time-harmonic wavepacket with amplitude and phase modulations occurring on the same

Address for correspondence: Professor Larry Redekopp, Department of Aerospace Engineering, University of Southern California, Los Angeles, CA 90089-1191.
*Present address: Météorologie Nationale CNRM, 42, avenue G. Coriolis, 31057 Toulouse Cedex, France.
†Present address: Département de Mécanique, Ecole Polytechnique, 91128 Palaiseau Cedex, France.

Published by Elsevier Science Publishing Co., Inc. 0022-2526/91/$3.50

length scale as the spatial inhomogeneities of the system. From a more mathematical point of view, its frequency and spatial distribution satisfy a linear eigenvalue problem involving the entire physical domain of interest. The main motivation for the study of such objects has been to demonstrate the possible existence of purely hydrodynamic resonances in spatially developing shear flows.

This type of description was first proposed by Koch [6] to explain the sharp selection of a definite wavenumber and frequency in the Karman vortex street behind bluff bodies at low Reynolds numbers. Similar ideas have been independently developed by Pierrehumbert [7] and Bar-Sever and Merkine [8] in the study of baroclinic instabilities in geophysical flows. The conjecture made by these authors is that hydrodynamic resonances, in other words temporally growing global modes, are due to the coexistence, within the same flow, of a region of local absolute instability and a region of local convective instability. These notions, first introduced in the study of plasma instabilities [9–12], allow one to differentiate, in a given reference frame, between the various responses of a *parallel flow* to localized disturbances. In convectively unstable flows, the amplitude of the linear response at a fixed point decays to zero, whereas it grows exponentially in time in absolutely unstable flows.

Resonances arising in shear flows have usually been described in terms of a feedback loop composed of hydrodynamic *vorticity* waves traveling downstream and far-field *acoustic* waves traveling upstream [13]. Examples include wake tones, jet tones, and edge tones, as reviewed by Rockwell and Naudascher [14]. In the present work, we wish to study a different class of resonance phenomena. The global modes of interest here are of a purely hydrodynamic nature: they only involve a combination of upstream and downstream vorticity waves in the shear region, without the need for irrotational acoustic fluctuations.

Local absolute/convective instability concepts lead to an appealing classification of spatially developing flows, provided one assumes that the length scale of streamwise inhomogeneities in the basic flow is much larger than a typical instability wavelength. In such circumstances, the absolute/convective nature of the locally parallel flow may be defined unambiguously at each streamwise station. For instance, incompressible spatially evolving mixing layers [15,16] and boundary layers [17] are locally convectively unstable everywhere. As a result, they exhibit a strong sensitivity to forcing [18]. In the absence of coherent external perturbations, measured spectra are broadband and one does not observe self-sustained oscillations associated with global modes. By contrast, wakes behind bluff bodies [6,19–24] and low-density jets [25–27] may support finite-amplitude limit-cycle states when part of the flow is absolutely unstable. Discrete frequency spectra are then obtained without applying external forcing, which is an indication of the existence of self-sustained global modes. Finally, there is an intermediate class of flows, for example homogeneous jets [4,5,28], where the basic profile is almost absolutely unstable, or where the region of absolute instability is too small. In such cases, the entire flow acts as a slightly damped resonator. Frequency spectra are broadband, but with a peak at a well-defined frequency.

It is impossible here to discuss the current state of the art in any detail. Review articles have appeared that treat the subject from a fluid-mechanical point of view [29,30]. The reader is referred to a recent extensive survey [31] for background information.

The goal of the present analysis is to present a general treatment of slowly diverging flows in the WKBJ approximation. We wish to establish the relationship between the *local* absolute/convective character of the instability and the *global* properties of the entire flow. Rigorous criteria are given for the existence of temporally growing resonances and for the value of the global-mode frequency. The entire study is restricted to media of infinite extent that are evolving in one spatial dimension only. The results are, however, equally applicable to two-dimensional flows, provided the cross-stream coordinate is an eigenfunction direction as in shear layers, jets, and wakes.

The paper is organized as follows. In Section 2, we recall essential definitions pertaining to local instability concepts in parallel flows, i.e., homogeneous media. The presentation of the main ideas is very incomplete: we only discuss aspects of the theory that are relevant to this investigation. More detailed accounts are given elsewhere, for instance in [31]. The properties of global modes are studied in Section 3. General concepts are introduced in Section 3.1, and second-order systems are analyzed in Section 3.2. The main results are summarized in three theorems and two corollaries. Relying on previous work, we briefly sketch how the analysis may be extended to systems of arbitrary order in Section 3.3. In the conclusion we review the most important results and compare them with related investigations of instabilities in specific spatially developing flows. As will become apparent, the approach adopted in the core of the study is very geometrical. An alternate derivation of Theorems 1 and 2, based on energy-integral methods, is briefly outlined in an Appendix.

2. Instability concepts in homogeneous media

Before proceeding to the case of spatially developing systems in Section 3, it is essential to recall the main ideas underlying classical instability theory in parallel flows, i.e., homogeneous media. As demonstrated in the sequel, the concept of causality will play a crucial role, as it allows a rigorous determination of the direction of energy propagation for various spatial waves. Furthermore, in both sections, one needs to use mappings in the complex plane extensively as well as contour-deformation arguments. This section will introduce these techniques in the setting of parallel flows.

Following Bers [12], we only consider systems in one space dimension which are governed by a nonlinear partial differential equation for a vector field $\Psi(x,t)$, where x and t denote the space and time coordinate respectively. The system admits a vector $\vec{\mu}$ of control parameters and a basic state solution Ψ_0. When the system is forced by a given source $\mathbf{S}(x,t)$, the vector of fluctuations $\vec{\psi}(x,t;\vec{\mu})$ around Ψ_0 satisfies the system of linear partial differential equations

$$D\left[-i\frac{\partial}{\partial x}, i\frac{\partial}{\partial t}; \vec{u}\right]\vec{\psi}(x,t;\vec{\mu}) = \mathbf{S}(x,t). \tag{1}$$

Let $\hat{\vec{\psi}}(k,t;\vec{\mu})$ be the Fourier transform of $\vec{\psi}(x,t;\vec{\mu})$ such that

$$\vec{\psi}(x,t;\vec{\mu}) = \frac{1}{(2\pi)^2}\int_F\int_L \hat{\vec{\psi}}(k,\omega;\vec{\mu})e^{i(kx-\omega t)}\,d\omega\,dk, \tag{2}$$

where k and ω are the wavenumber and frequency respectively, and F and L are suitably chosen contours as discussed below. The function $\hat{\vec{\psi}}$ must then obey the equation

$$D[k,\omega;\vec{\mu}]\hat{\vec{\psi}}(k,\omega;\vec{\mu}) = \hat{\mathrm{S}}(k,\omega). \tag{3}$$

When $D[k,\omega;\vec{\mu}]=0$, one obtains the dispersion relation between k and ω. In general both k and ω are allowed to be complex, and one should determine the subset of values of k and ω which acquire physical meaning.

It is important to bear in mind the subtle difference that exists between time t and space coordinate x as a result of the *causality* assumption. Starting the "experiment" at a given instant, say $t=0$, breaks the symmetry $t \to -t$, and the causality condition stipulates that no response should be observed before $t=0$. Thus, the dispersion relation D should have the property sketched in Figure 1. Namely, for any path F in the complex k-plane connecting $k_r = -\infty$ to $k_r = +\infty$ with k_i bounded, there exists a corresponding path L in the complex ω-plane, with similar characteristics to F, that lies above all the zeros and singularities of D when k travels along F. In other words, a physically acceptable dispersion relation should respect the following property:

$$\omega_{i,\max} \equiv \max_{k_r}\{\omega_i | D[k,\omega;\vec{\mu}]=0\} \text{ exists for } k_i \text{ finite.} \qquad \text{(Property 1)}.$$

The proof of the above statement follows from the fact that $\hat{\vec{\psi}}$ is the Fourier transform of $\vec{\psi}$. For a causal source S, the response is given by

$$\vec{\psi}(x,t;\vec{\mu}) = \frac{1}{(2\pi)^2}\int_F\int_L \frac{\hat{\mathrm{S}}(k,\omega)}{D[k,\omega;\vec{\mu}]}e^{i(kx-\omega t)}\,d\omega\,dk. \tag{4}$$

The source S is causal, and its Fourier transform $\hat{\mathrm{S}}(k,\omega)$ should have no singularities in the complex ω-plane located above a path L that depends on F. Since one needs $\vec{\psi}=0$ when $t<0$, the dispersion relation should therefore satisfy Property 1.

For convenience and clarity of presentation, the analysis and discussion to follow considers scalar systems exclusively. However, the conclusions of this study are not affected by this restriction and are believed to apply to a wide class of spatially developing evolution systems.

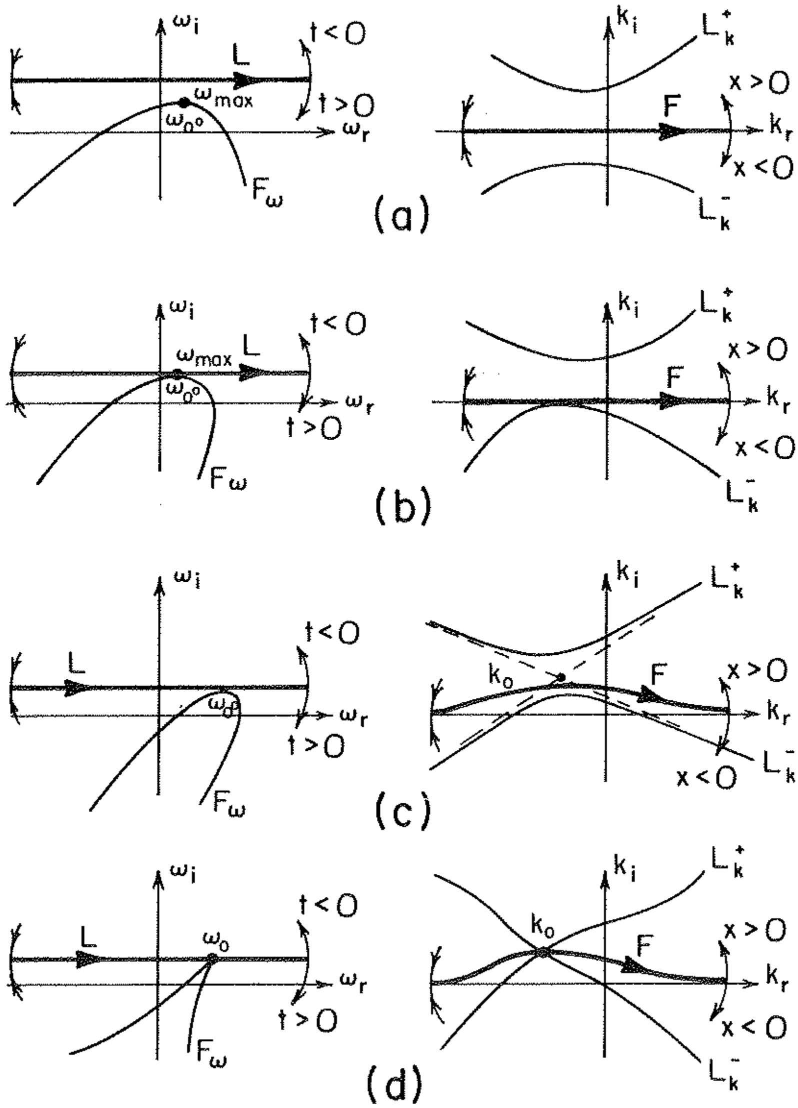

Figure 1. Integration contours L and F, temporal and spatial branches in complex k and ω planes. Temporal branch $\omega(k)$, k on F, is denoted by F_ω. Spatial branches $k^+(\omega), k^-(\omega)$, ω on L, are denoted by L_k^+ and L_k^-. (a), (b), (c), and (d) refer to different stages of the pinching process. In (d) F is pinched by L_k^+ and L_k^-.

2.1. Temporal stability theory

It is well established that temporal stability theory corresponds to the time evolution of a given real wavenumber k over all space. For simplicity, we shall assume in the rest of this section that there is at most one unstable temporal branch $\omega(k)$. According to Property 1, temporal modes in the complex ω-plane

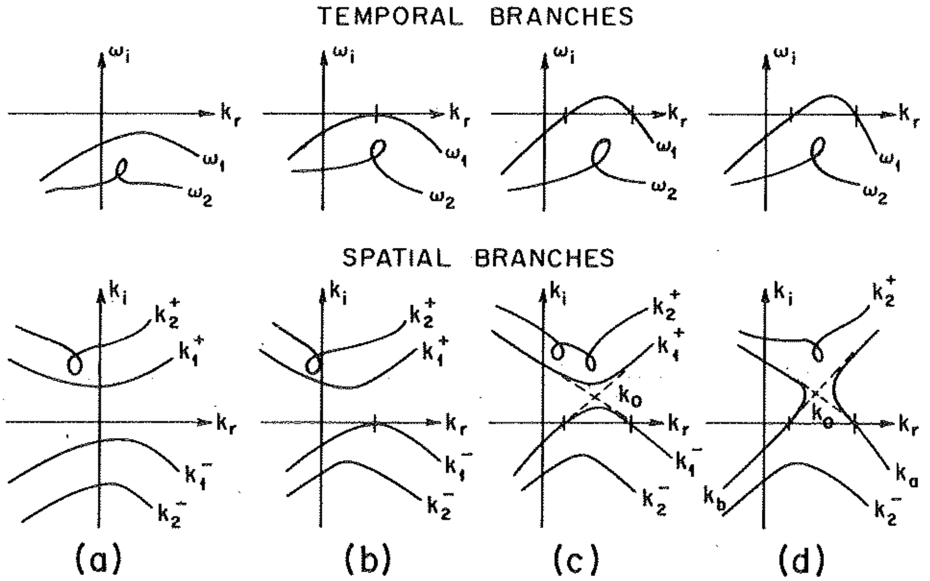

Figure 2. Temporal modes $\omega_i(k)$, k real, and spatial branches $k(\omega)$, ω real in k-plane: (a) stable case; (b) neutrally stable case; (c) convectively unstable case; (d) absolutely unstable case.

are bounded in the ω_i-direction, and there is, at a particular real wavenumber $k_{\max}$, a well-defined maximum growth rate $\omega_{i,\max}$ with corresponding frequency $\omega_{r,\max}$. The system is then said to be stable if $\omega_{i,\max} < 0$, neutrally stable if $\omega_{i,\max} = 0$, and unstable if $\omega_{i,\max} > 0$. Different possible cases are displayed in Figure 2 for situations in which no specific discrete symmetry prevails. As a control parameter, say the Reynolds number or Rayleigh number, is increased, the temporal instability characteristics may change as illustrated in the sequence of sketches in Figure 2.

2.2. *Spatial stability theory*

In contrast to temporal stability theory, one may require ω to be real and obtain spatial branches $k(\omega)$ in the complex k-plane which represent spatially amplifying or decaying waves. Typical configurations have been sketched in the lower part of Figure 2. Since there is no equivalent of Property 1 in the k-plane, the sign of $-k_i(\omega)$ fails to provide any clue regarding the stable or unstable nature of the flow. In fact, one does not know *a priori* the direction in which the energy of a particular branch $k(\omega)$ will "propagate." One may understand, at an intuitive level, the relationship between the character of the instability and the shape of the spatial branches by following the sequence of sketches in the lower half of Figure 2. When the system is stable [Figure 2(a)] there should be no amplified spatial waves. This implies that the branches $k^+(\omega)$ lying in the upper half plane "propagate" to the right $x > 0$, whereas the branches $k^-(\omega)$ lying in the lower half plane "propagate" to the left $x < 0$. Neither branch can cross from one side of the k_r-axis to the other and remain there indefinitely as the frequency ω is varied. A + and − label and corresponding "propagation" directions can be assigned to the continuously deforming branches as the system becomes neutrally stable [Figure 2(b)] and unstable [Figure 2(c)].

This continuity argument is, however, no longer tenable when two spatial branches emanating from opposite sides collide as shown in Figure 2(d). In such a case, spatial branches switch and the system undergoes a transition from convective instability [Figure 2(c)] to absolute instability [Figure 2(d)]. The following definitions may then be introduced. A flow is said to be *stable* if each individual spatial branch $k(\omega)$, ω real, solely belongs to one side of the k_r-axis. It is said to be *convectively unstable* when one of the spatial branches crosses the k-axis. Finally, the flow becomes *absolutely unstable* when spatial branches originating from distinct sides of the k_r-axis collide. The collision point k_0 is a saddle of $\omega(k)$, and the corresponding *absolute frequency* ω_0 is in general a branch point of $k(\omega)$. In the complex ω-plane the transition between convective and absolute instability is signaled by the fact that the absolute frequency ω_0 has crossed the ω_r-axis. The criterion for absolute instability is therefore that $\omega_{0,i}$ be positive.

2.3. *Signaling problem*

A more rigorous proof of the above criterion follows from a study of the signaling problem. In this case, Equation (3) is solved for a pointwise time-harmonic source of real frequency ω_f. In the inverse Fourier transform (4), the source term takes the form $\hat{S}(k,\omega) \propto 1/(\omega - \omega_f)$, and the configuration of the integration paths L and F is sketched in Figure 1. The temporal mode $\omega(k)$ maps F into F_ω, and the spatial branchess $k(\omega)$ map L into L_k^+ and L_k^-. According to Property 1, when L is high enough, F can be made to coincide with the k_r-axis without intersecting any of the spatial branches L_k^+ and L_k^- [Figure 1(a)]. In the range $x < 0$ ($x > 0$), F is closed by a semicircle at infinity in the lower (upper) half k-plane, and this procedure naturally selects the L_k^- and L_k^+ branches pertaining to $x < 0$ and $x > 0$, respectively. When L is lowered [Figure 1(b), (c)], F must be deformed to avoid crossing the spatial branches. This is possible until two spatial branches that were initially on distinct sides of the k_r-axis pinch the contour F [Figure 1(d)]. If pinching takes place before L reaches the ω_r-axis, as in Figure 1(d), no + and − branches can be defined for $\omega = \omega_f$ real. The system is then absolutely unstable. By comparing Figure 1(b) and (d), one obviously has the inequality

$$\omega_{0,i} \leq \omega_{i,\max}. \tag{5}$$

The absolute growth rate is necessarily bounded from above by the maximum temporal growth rate.

2.4. *Impulse response*

The physical implications of absolute/convective instability concepts are more readily accessible when one examines the impulse response, or Green's function, of a system that is subjected to a localized input in both space and time. As

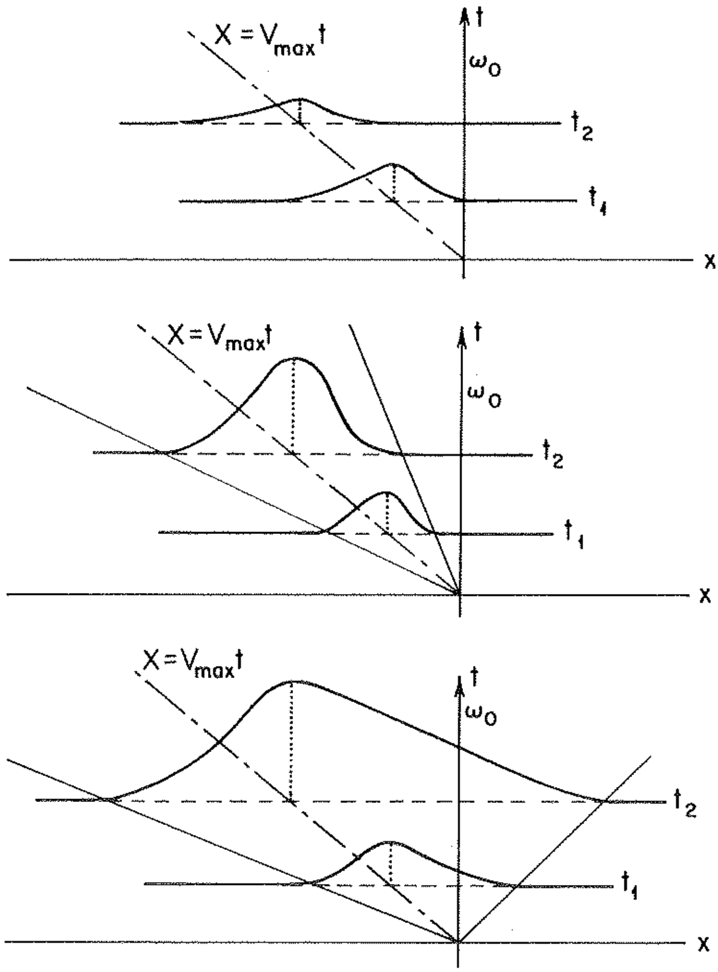

Figure 3. Impulse response in homogeneous media: (a) stable; (b) convectively unstable; (c) absolutely unstable.

discussed in earlier reviews, for instance [9–12, 29, 31], the response takes the form of a wave packet in the x-t plane (Figure 3). Along a given ray $x/t = V$, the instability selects a frequency-wavenumber pair $\omega^*(V), k^*(V)$ given by the group velocity

$$\frac{\partial \omega}{\partial k}[k^*(V)] = V. \tag{6}$$

The maximum growth rate $\omega_{i,\max}$ is observed along the specific ray

$$V_{\max} = \frac{\partial \omega}{\partial k}(k_{\max}),$$

which can be viewed as the characteristic velocity of the center of the wavepacket. At the fixed source location, one detects instead the particular pair ω_0, k_0 corresponding to the solution of (6) with $V = 0$. Thus, the maximum growth rate $\omega_{i,\max}$ pertains to the temporal evolution of the instability in a frame of reference moving with the wavepacket, whereas the absolute growth rate $\omega_{0,i}$ measures the growth or decay of the impulse response in a fixed reference frame attached to the source. The three different impulse responses illustrated in Figure 3(a),(b),(c) correspond to stable, convectively unstable, and absolutely unstable situations, respectively. It can be concluded that, in an absolutely unstable medium, any transients will progressively overwhelm the response to external perturbations. In such cases, the signaling problem becomes meaningless.

3. Global modes in infinite spatial domains

3.1. General concepts

The goal of this section is to study the properties of infinitesimal linearized disturbances in a medium that is of infinite extent and spatially developing in x. In other words, in the class of problems under consideration, invariance with respect to translations $x \to x + \text{const}$ no longer holds, but time invariance $t \to t + \text{const}$ persists. Thus, one seeks *global-mode* solutions with a temporal behavior of the form $e^{-i\omega_G t}$, where ω_G is an unknown complex global frequency. Global modes with a positive value of $\omega_{G,i}$ are of particular interest, since they lead to a temporal instability of the entire spatially developing system. The determination of global modes typically involves solving an eigenvalue problem that must be examined on a case-by-case basis unless additional assumptions are made. We recall that the main goal of our study is to relate local and global instability properties. In order to make this connection possible, it is necessary to assume that the length scale characterizing the spatial inhomogeneities of the medium is much larger than a typical instability wavelength. Under such conditions the local instability properties introduced in the previous section are unambiguously defined at each station on a locally parallel basis. In particular, one may calculate local quantities $\omega_{\max}(x)$, $\omega_0(x)$, etc., as if the system were locally homogeneous in x. Thus, in a given spatially evolving system, distinct regions of local stability and local instability may coexist. Furthermore, within the unstable region, one differentiates between locally convectively unstable and locally absolutely unstable domains. The local nature of the instability dictates the behavior of the *short-time* response to an impulse within a given region. Nonetheless, it should be emphasized that local properties give no insight into the *long-time* impulse response of the entire spatially varying system.

The parallel-flow considerations outlined in Section 2 have demonstrated the importance of causality in the correct assignment of spatial branches. In the same spirit, one must only pay attention to global-mode solutions which are the final outcome of an "experiment" initiated, say, at $t = 0$. To understand the role played by causality in the choice of boundary conditions at $x = \pm\infty$, we very temporarily restrict the discussion to infinite systems that possess only a finite region of local instability in x, the medium being locally stable at $\pm\infty$. In such circumstances, causality requires that no fluctuation energy propagate from infinity towards the bulk, and, as a result, one must impose the condition that the perturbation field vanishes at $x = \pm\infty$. The assumption of local stability in the neighborhood of $x = \pm\infty$ is, however, unduly restrictive. The above argument may be extended to situations where the medium has a finite region of absolute instability, allowing for possible convective instability in the vicinity of $x = \pm\infty$. In this more general configuration, one can still determine the "propagation" direction of all spatial waves in the convectively unstable domains near infinity, provided $\omega_{G,i} > 0$, by making use of the analysis of Section 2. We choose to focus on a single pair of spatial branches that exhibit switching in the bulk of the medium, as detailed in the next sections. For a given value of ω, the spatial branch selected near $x = +\infty$ (respectively, $x = -\infty$) is then taken to be causal and therefore subdominant near $x = +\infty$ (respectively, $x = -\infty$). In the present context, "*subdominant*" refers to the solution that is exponentially small with respect to the other. Causality considerations then lead to a singular boundary-value problem on $-\infty < x < +\infty$, and in general global-mode eigenfunctions will be obtained for only discrete complex values of ω_G. The condition that fixes the possible values of ω_G must be obtained by connecting the subdominant branches at $+\infty$ and at $-\infty$ in the bulk of the medium. The key phenomenon is therefore the manner in which *branch switching* takes place between a left-moving wave at $-\infty$ and a right-moving wave at $+\infty$. These waves will be spatially attenuated if $\omega_{G,i} > 0$ and the regions near both infinities are locally stable. They will only be subdominant if these same regions are convectively unstable.

There is a very close correspondence between the global modes of the present study and bound states in potential-well problems. It is well established in the literature on quantum mechanics [32–37] and from earlier work by Stokes that the correct way to treat branch switching is to immerse the physical problem into the complex x-plane. A naive analysis restricted to real x will necessarily miss contamination by exponentially small terms that may, in some region, become dominant. Branch switching will, in general, occur at some points in the complex x-plane, and this phenomenon will make itself felt everywhere, particularly on the real x-axis.

3.2. *Second-order systems*

The simplest possible "parallel flow" displaying a saddle point in the complex k-plane involves a dispersion relation that is linear in ω and quadratic in k of the form

$$D[k, \omega; \mu] \equiv i\omega - \sigma k^2 + ipk + q. \tag{7}$$

In physical space, the dispersion relation (7) is associated with the linear differential operator

$$D\left[-i\frac{\partial}{\partial x}, i\frac{\partial}{\partial t}; \mu\right] \equiv -\frac{\partial}{\partial t} + \sigma\frac{\partial^2}{\partial x^2} + p\frac{\partial}{\partial x} + q. \tag{8}$$

In the spatially evolving case, the coefficients are taken to be functions of the spatial coordinate x, and one must then solve a generalized linear Ginzburg-Landau equation

$$\psi_t = \sigma(x)\psi_{xx} + p(x)\psi_x + q(x)\psi. \tag{9}$$

Local instability properties are readily obtained by inspection. The maximum temporal growth rate is

$$\omega_{i,\max} = q_r + \frac{p_i^2}{4\sigma_r}, \tag{10}$$

and the absolute wavenumber and frequency are given by

$$k_0 = \frac{ip}{2\sigma}, \qquad \omega_0 = i\left(q - \frac{p^2}{4\sigma}\right). \tag{11}$$

If one sets

$$\sigma = \frac{i\omega_{kk}}{2}, \tag{12}$$

one must necessarily have

$$\omega_{kk,i} < 0, \tag{13}$$

in order to satisfy causality. This condition corresponds to the existence of a high-wavenumber cutoff in the temporal stability problem. It is assumed that (13) holds in the entire complex x-plane and that ω_{kk} is an analytic function of x everywhere. We shall not attempt to relax this assumption here.

According to the definition of global modes given previously, time-harmonic solutions are sought with variations of the form $\psi(x,t) = \phi(x;\omega_G)e^{-i\omega_G t}$, ω_G complex. Furthermore, these solutions must become subdominant as x goes to $+\infty$ and $-\infty$. The governing equation for the eigenfunction $\phi(x;\omega_G)$ is

$$-i\omega_G\phi = \sigma(x)\phi_{xx} + p(x)\phi_x + q(x)\phi, \tag{14}$$

and, through the change of function

$$\phi(x) = \phi^*(x)\exp\left[-\frac{1}{2}\int^x \frac{p(x)}{\sigma(x)}\,dx\right], \tag{15}$$

Equation (14) reduces to the compact form

$$\phi^*_{xx} + Q(x)\phi^* = 0, \tag{16}$$

with

$$Q(x) \equiv \frac{1}{\sigma(x)}\left(i\omega_G + q - \frac{p^2}{4\sigma}\right) - \frac{1}{2}\left(\frac{p}{\sigma}\right)_x. \tag{17}$$

Thus, if one defines the shifted absolute frequency

$$\tilde{\omega}_0(x) \equiv \omega_0 - \tilde{\omega}_0(x) \equiv \omega_0 - \sigma(k_0)_x, \tag{18}$$

the coefficient $Q(x)$ appearing in (16) can simply be written as

$$Q(x) = 2\frac{\omega_G - \tilde{\omega}_0(x)}{\omega_{kk}(x)}. \tag{19}$$

It is convenient to explicitly display the WKB parameter ϵ defined as the ratio between a typical instability wavelength and the length scale associated with spatial inhomogeneities of the system. Let $X = \epsilon x$ be the corresponding slow-scale variable. Equation (16) may then be recast in the form

$$\epsilon^2 \phi^*_{XX} + Q(X)\phi^* = 0, \tag{20}$$

with

$$Q(X) \equiv 2\frac{\omega_G - \tilde{\omega}_0(X)}{\omega_{kk}(X)} \tag{21}$$

and

$$\tilde{\omega}_0(X) = \omega_0(X) - \tilde{\omega}_0(X) = \omega_0(X) - \epsilon\sigma(X)[k_0 X]_X. \tag{22}$$

The eigenvalue problem for ω_G and ϕ^* specified by (20) and the boundary conditions at $X = \pm\infty$ also arises in the motion of a quantum particle in a potential well. According to standard WKBJ approximation theory, the two independent solutions of (20) admit, in the limit $\epsilon \to 0$, asymptotic expansions of the form $[Q(X)]^{-1/4}\exp\{\pm(i/\epsilon)\int\sqrt{Q(X)}\,dX\}$. Following Titshmarsh [32], Pokrovskii and Khalatnikov [33], Wasow [34], Hille [35,36] and Bender and Orszag [37], we introduce the mapping from the complex X-plane to the complex Z-plane defined by

$$Z = \frac{1}{\epsilon}\int^X \sqrt{Q(X)}\,dX. \tag{23}$$

As seen by inspection of (23), the asymptotic solutions are multiple-valued, and branch cuts of $Z(X)$ have to be chosen at the branch points associated with the zeros of $Q(X)$. Since $Q(X)$ is analytic, the exact solutions of (20) are also analytic. The branch-point singularities appearing in the *approximate* solutions are therefore an artifact of the WKBJ method. As a consequence, the expansion of a given solution must change as X circles around a zero of $Q(X)$. This peculiar feature of WKBJ approximation schemes is commonly referred to as the *Stokes phenomenon*. It must be analyzed in detail before proceeding with the calculation of the eigenvalues and eigenfunctions.

The set of level curves $\operatorname{Im} Z = \text{const}$ are called *indicatrices*. The topology of the network of indicatrices plays a crucial role in the proper derivation of global mode characteristics. A single indicatrix passes through *regular* points of $Q(X)$, whereas several indicatrices join at *turning points*, i.e., zeros of $Q(X)$. The indicatrices are uniquely defined, but the label of each curve depends on the choice of branch cut and reference point in the integral (23). If X_0 is a particular turning point, the *Stokes lines* emerging from X_0 are the particular indicatrices uniquely defined by

$$\operatorname{Im} Z \equiv \operatorname{Im} \frac{1}{\epsilon} \int_{X_0}^{X} \sqrt{Q(X)}\, dX = 0. \tag{24}$$

The terminology varies from author to author. We have adopted here the definition employed by Bender and Orszag [37]. Across a Stokes line, transcendentally small terms may become exponentially large and the leading-order asymptotic expansion of a given solution may change. The set of Stokes lines define open domains D_j in the complex X-plane. If β_j is an integer taking one of the values $+1$ or -1, the two independent solutions in D_j will be asymptotic to

$$\frac{1}{[Q(X)]^{1/4}} \exp\left\{ i \frac{\beta_j}{\epsilon} \int_{X_0}^{X} \sqrt{Q(X)}\, dX \right\}$$

and

$$\frac{1}{[Q(X)]^{1/4}} \exp\left\{ - i \frac{\beta_j}{\epsilon} \int_{X_0}^{X} \sqrt{Q(X)}\, dX \right\}$$

respectively. If the first expression is exponentially larger than the second expression, it is said to be the *dominant* WKBJ approximation in this sector. The other expression is then the *subdominant* WKBJ approximation. The following rules are applicable [37]:

1. If a solution is asymptotic, in some domain D_j, to the *subdominant* approximation, then the same approximation remains valid in all the *neighboring* domains (i.e., those which share with D_j a common boundary not reducible to a single point).
2. If a solution is asymptotic, in some domain D_j, to the *dominant* approximation, nothing can be said regarding the approximation in neighboring domains.

This fundamental property has strong implications for the global-mode problem. Since we are interested in subdominant solutions at $X_r = \pm\infty$, the negative X_r-axis and the positive X_r-axis must belong to domains D_j that do not share a common boundary. The following lemma is then a direct consequence of the above considerations.

LEMMA 1: *To avoid exponentially large terms as* $|X_r| \to \infty$, *the deformed contours of the* X_r*-axis must cross at least two Stokes lines that are connected at one or several turning points.*

In the ensuing development we shall need to know the sign of $\mathrm{Im}\{[\omega_G - \tilde{\omega}_0(X)]/\omega_{kk}(X)\}$ as X travels along a given horizontal path M in the complex X-plane. We shall assume that $\omega_{kk,i}(X) < 0$ and that $\tilde{\omega}_{0,i\max} \equiv \max_{X \in M}\{\tilde{\omega}_{0,i}(X)\}$ exists. The results are summarized in the next lemma.

LEMMA 2: *If* $\omega_{G,i} > \tilde{\omega}_{0,i\max}$, *the branch cut of* $Z'(X) \equiv (1/\epsilon)\{2[\omega_G - \tilde{\omega}_0(X)]/\omega_{kk}(X)\}^{1/2}$ *may be chosen so that* $\mathrm{Im}\, Z'(X)$ *remains positive on M.*

We shall require the branch cut not to cross M. Under these conditions, along any straight-line M parallel to X_r, the function

$$\mathrm{Im}\, Z(X) \equiv \mathrm{Im}\, \frac{1}{\epsilon} \int \sqrt{2 \frac{\omega_G - \tilde{\omega}_0(X)}{\omega_{kk}(X)}}\, dx$$

increases monotonically as X travels along M from $-\infty$ to $+\infty$. Thus M crosses indicatrices with the same label only once. There are, in particular, no contours M crossing two or more connected Stokes lines. It can be concluded from Lemma 2 that, when $\omega_{G,i} > \tilde{\omega}_{0,i\max}$, the real X_r-axis crosses at most one Stokes line. Application of Lemma 1 then excludes the existence of global modes, and the following theorem holds.

THEOREM 1: *A system will have no global modes with a growth rate* $\omega_{G,i}$ *greater than* $\tilde{\omega}_{0,i\max}$. *Thus, one must have*

$$\omega_{G,i} \leq \tilde{\omega}_{0,i\max}. \tag{25}$$

This result establishes a relationship between local and global instability properties. In the WKBJ approximation, $\tilde{\omega}_{0,i\max}$ differs from $\omega_{0,i\max}$ by an order-ϵ correction term [see Equation (22)]. If ω_g denotes the leading-order approximation, in the WKBJ sense, of the global-mode frequency,

$$\omega_G = \omega_g + O(\epsilon), \tag{26}$$

one obtains the following important corollary:

COROLLARY 1: *The leading-order approximation* ω_g *to the global-mode frequency satisfies the inequality*

$$\omega_{g,i} \leq \omega_{0,i\max} + O(\epsilon). \tag{27}$$

As a result, a system nowhere absolutely unstable ($\omega_{0,i\max} < 0$) cannot sustain global modes with an $O(1)$ temporal growth rate.

Note that, on account of the $O(\epsilon)$ difference between $\tilde{\omega}_{0,i\max}$ and $\omega_{0,i\max}$, weakly growing global modes cannot be excluded in purely convectively unstable systems when $\omega_{0,i\max}$ is very small. It is also important to notice that absolute instability is only a necessary condition for strong global instability. Examples exist [1–5] where the medium is absolutely unstable in a finite domain, but nonetheless globally stable.

It is possible to be considerably more specific if additional assumptions are made regarding the mapping $\tilde{\omega}_0(X)$ from the X-plane to the ω-plane. In general $\tilde{\omega}_0(X)$ is single-valued, whereas the inverse map $\tilde{\omega}_0^{-1}$ is multiple-valued. Anticipating needs in the derivations that will follow, we assume that the complex ω-plane is composed of at least two Riemann sheets with a branch point in common. Correspondingly, level contours of $\tilde{\omega}_{0,i}(X)$ admit a saddle point in the complex X-plane. The reader will have immediately drawn the analogy between the present assumptions and those commonly made in the presentation of absolute/convective instability concepts for parallel flows. Here the X-plane plays, in some sense, the role of the k-plane in Section 2. Indeed, the arguments to be used will share some features with those applied in specifying the integration path in the k-plane. To be more specific, the following assumptions are made:

Assumption 1. The map $\tilde{\omega}_0(X)$ is single-valued and holomorphic in a strip centered on the real X-axis, and the first singular point is a *saddle point* $\tilde{X}_s$ such that

$$\frac{d\tilde{\omega}_0}{dX}(\tilde{X}_s) = 0.$$

The middle portion of the X_r-axis is on a hill of the saddle, i.e., its "altitude" expressed in terms of $\tilde{\omega}_{0,i}$ is higher than $\tilde{\omega}_{s,i} \equiv \operatorname{Im} \tilde{\omega}_0(\tilde{X}_s)$.

Assumption 2. $\tilde{\omega}_{0XX,i}(\tilde{X}_s) < 0$.

The latter restriction is the analogue of the high-wavenumber cutoff requirement $\omega_{kk,i} < 0$ adopted in Section 2. It might be possible to relax this assumption on a case-by-case basis, but we shall not attempt to do so here. We are now in a position to state a second important theorem regarding the characteristics of global modes.

THEOREM 2. *Under Assumptions* 1 *and* 2, *there are no global-mode solutions with a temporal growth rate* $\omega_{G,i}$ *greater than* $\tilde{\omega}_{s,i}$. *In other words*

$$\omega_{G,i} \leq \tilde{\omega}_{s,i}. \tag{28}$$

Proof of Theorem 2: The derivation of Theorem 2 relies on contour-deformation arguments which bear a strong similarity with those of Section 2. Let M be a horizontal path in the complex X-plane, and M_ω its image in the complex

ω-plane under the map $\tilde{\omega}_0(X)$ (see Figure 4). When M coincides with the X_r-axis, its image M_ω is necessarily bounded in the ω_i-direction as shown in Figure 4(a). This results from the assumption made in Lemma 2 regarding the existence of $\tilde{\omega}_{0,i\,\max} \equiv \max_{X \in M_\omega}\{\tilde{\omega}_{0,i}(X)\}$. Conversely, if L is a straight horizontal line in the ω-plane, its image in the complex X-plane will be composed of several branches L_j^{-1}. If L is chosen high enough so as not to cross M_ω, the contour M will not cross any of the branches L_j^{-1} either [Figure 4(a)]. It may be the case that, for some L, the branches L_j^{-1} are all located on one side of M.

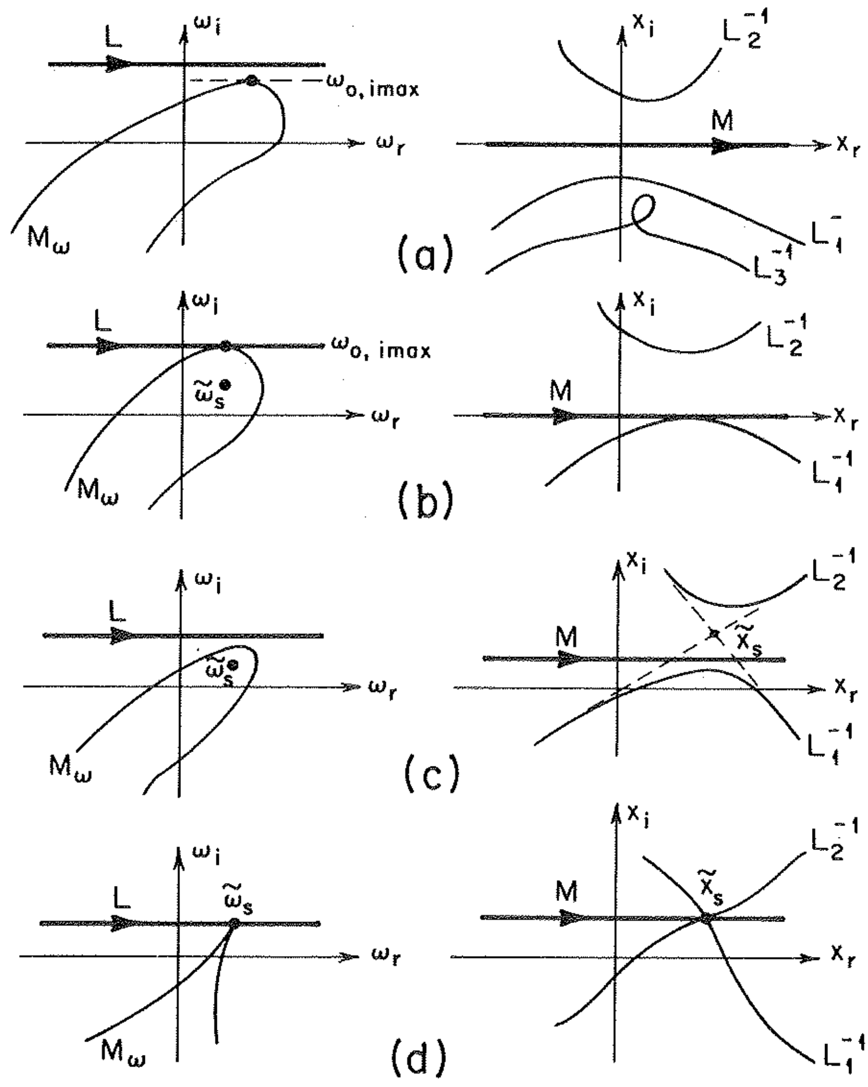

Figure 4. Contours M and L in complex X and ω-planes. The image of M under the map $\omega_0(X)$ is M_ω. The image of L under the inverse map ω_0^{-1} has several branches L_j^{-1}, $j = 1, 2, 3, \ldots$. (a), (b), (c), and (d) refer to different stages of the pinching process. In (d) M is pinched by L_1^+ and L_2^-.

However, on account of Assumption 1, branches are bound to appear on the other side of M as soon as L is sufficiently close to the saddle point $\tilde{X}_s$. For simplicity, we assume that the two branches L_1^{-1} and L_2^{-1} which will pinch at the saddle $\tilde{X}_s$ are already present. According to Assumption 2, the locations of L_1^{-1} and L_2^{-1} are such that

$$\max\{\mathrm{Im}\, X | X \in L_1^{-1}\} < \min\{\mathrm{Im}\, X | X \in L_2^{-1}\}. \tag{29}$$

The initial positions of L and M and their images are sketched in Figure 4(a) with L above the maximum $\tilde{\omega}_{0,i\max}$. We recall that, according to Lemma 2 and its consequences, the function $Z(X)$ is montonic on M when $\omega_{G,i} > \tilde{\omega}_{0,i\max}$. Thus M can only cross *one Stokes line*. We conclude that the global-mode frequency does not lie on a contour L of the type shown in Figure 4(a). As L moves downward, it will eventually reach a point where $\omega_{G,i} = \tilde{\omega}_{0,i\max}$ as sketched in Figure 4(b). At this stage, only one branch, say L_1^{-1}, will touch the contour M. To avoid contact, one only needs to translate M upward or downward by a small amount. As Lemmas 1 and 2 remain valid for any path M parallel to the X_r-axis, the previous reasoning still holds and L does not include any possible global-mode frequencies. One may continue to lower L and translate M so as to avoid contact with L_1^{-1} until the saddle point $\tilde{X}_s$ is reached [Figure 4(c),(d)]. When M is pinched, it cannot avoid the contours L_j^{-1} any longer and a cusp develops at ω_s on L. Thus, until L reaches the frequency $\tilde{\omega}_s$ of the "closest" saddle point, it is pointless to seek a global-mode frequency on L. This proves the theorem.

Theorem 2 also establishes a relationship between local and global instability properties that can be immediately stated in the following corollary.

COROLLARY 2. *Under Assumptions* 1 *and* 2, *the leading-order approximation to the global-mode frequency* ω_g *satisfies the inequality*

$$\omega_{g,i} \le \omega_{s,i} + O(\epsilon), \tag{30}$$

where $\omega_s = \omega_0(X_s)$ *is the complex absolute frequency at the saddle point* X_s *such that* $(d\omega_0/dX)|_{X_s} = 0$.

Remarks:

1. It is assumed in Figure 4 that $\tilde{X}_{s,i}$ is positive, but the same reasoning holds when $\tilde{X}_{s,i}$ is negative.
2. Assumption 2 is essential to the argument of the proof. If it is relaxed, pinching may take place sideways as illustrated in Figure 5. Parts of M can always be deformed so as to avoid approaching branches. Nevertheless, once M is no longer a straight horizontal line, it is not legitimate to invoke Lemma 2 in order to prove the monotonicity of Z.
3. According to Figure 4, it is clear that one necessarily has $\omega_{s,i} \le \omega_{0,i\max}$, and Theorem 2 and Corollary 2 provide an upper bound for the temporal growth rate of global modes that is much sharper than $\omega_{0,i\max}$ given by Theorem 1 and Corollary 1.

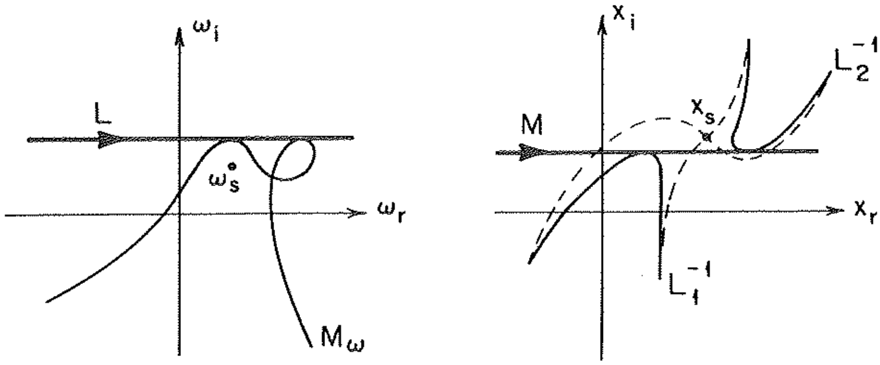

Figure 5. Sketch illustrating pathological case of "sideways pinching." This situation is excluded.

A definite statement can now be made regarding the existence of global modes and the value of the dominant global frequency.

THEOREM 3. *Under Assumptions 1 and 2, the temporal growth rate of global modes is given to leading order in the WKBJ approximation by the upper bound* $\omega_{s,i}$. *An estimate of the corresponding complex global frequency is* ω_s.

Proof of Theorem 3: Let us assume that the expansion of ω is of the form

$$\omega_G = \tilde{\omega}_s + \epsilon\tilde{\omega}_2 + O(\epsilon^2), \tag{31}$$

where $\tilde{\omega}_s \equiv \tilde{\omega}_0(\tilde{X}_s)$, and demonstrate that one thereby satisfies all the constraints of the eigenvalue problem. Since $\tilde{X}_s$ is a saddle point, the function $\tilde{\omega}_0(X)$ admits a Taylor series expansion

$$\tilde{\omega}_0(X) = \tilde{\omega}_s + \frac{\tilde{\omega}_{0XX}}{2}(X - \tilde{X}_s)^2 + O(X - \tilde{X}_s)^3, \tag{32}$$

with $\tilde{\omega}_{0XX} = O(1)$. We then define an inner region of size $\epsilon^{1/2}$ around the turning point X_s and introduce the corresponding inner variable $z = \epsilon^{-1/2}(X - \tilde{X}_s)$. The inner problem can be written in the form

$$\phi^*_{zz} - \left[-\frac{2\tilde{\omega}_2}{\omega_{kk}} + az^2 + \epsilon g_1(z)\right]\phi^* = 0, \tag{33}$$

where $a = \tilde{\omega}_{0XX}/(\omega_{kk}) = O(1)$ and $g_1(z)$ is an $O(1)$ holomorphic function. The configuration of Stokes lines in the vicinity of $\tilde{X}_s$ is sketched in Figure 6. We recall that, in order to satisfy the boundary conditions, subdominant solutions are required in the outer sectors containing $X_r = \pm\infty$. The role of the turning-point inner region is to allow "smooth" switching from one subdominant solution in one sector to another subdominant solution in the other sector. Following standard methods, one may identify the leading-order terms in (33)

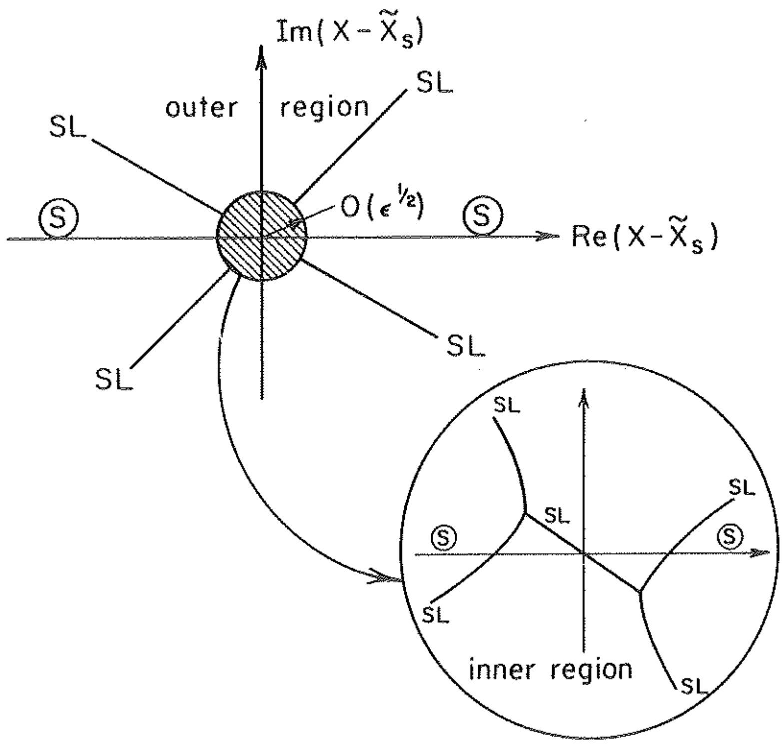

Figure 6. Structure of inner region around saddle point $\tilde{X}_s$ including topology of surrounding Stokes lines (SL = Stokes lines; S = subdominant).

with the parabolic cylinder equation. Matching of the inner solutions with the outer subdominant solutions requires that $\tilde{\omega}_2$ take the discrete values

$$\tilde{\omega}_2 = (2n+1)\left(\frac{\tilde{\omega}_{0XX}\omega_{kk}}{4}\right)^{1/2}, \tag{34}$$

n being any positive or zero integer and the branch cut of the square root being taken on the negative real axis. According to Equation (13) and Assumption 2, $\arg \omega_{kk}$ and $\arg \tilde{\omega}_{0XX}$ both belong to the same range $]-\pi, 0[$, and one immediately concludes that $\tilde{\omega}_{2,i} < 0$. Thus, under Assumptions 1 and 2, there is a discrete infinity of global modes, and the most unstable has a complex frequency given by $\tilde{\omega}_s$, to dominant order in the WKBJ approximation. Finally, we note that $\tilde{\omega}_s$ differs from ω_s by an $O(\epsilon)$ quantity [see Eq. (22)], and we can state that the saddle-point frequency $\omega_s = \omega_0(X_s)$ provides the dominant-order estimate of the global frequency. This completes the proof of the theorem.

Combining (31) and (34), one obtains the following discrete spectrum of global frequencies:

$$\omega_n \sim \tilde{\omega}_s + \frac{2n+1}{2}\epsilon(\tilde{\omega}_{0XX}\omega_{kk})^{1/2}. \tag{35}$$

It is somewhat remarkable that the global-mode characteristics admit WKBJ approximations involving only *local* instability properties of the spatially developing medium around the saddle point X_s where $d\omega_0/dX = 0$.

3.3. *Extension to n th-order systems*

Theorems 1, 2, and 3 and their corollaries have been derived in the context of linear second-order differential operators. One still needs to establish whether the results remain valid for arbitrary differential systems of the form

$$D\left[-i\frac{\partial}{\partial x}, i\frac{\partial}{\partial t}; \mu(x)\right]\psi(x,t) = 0, \tag{36}$$

where D is a linear differential operator defining, when μ is made constant, a dispersion relation at the relevant location x. The general idea consists in studying a class of systems in which branch switching implicates only a single pair of left-moving and right-moving waves, all other branches playing no role whatsoever.

As before, we seek global-mode solutions of the form $\psi(x,t) = \phi(x,\omega_G)e^{-i\omega_G t}$, with $\phi(x,\omega_G)$ satisfying the linear differential equation

$$D\left[-i\frac{\partial}{\partial x}, \omega_G; \mu(x)\right]\phi(x,\omega_G) = 0. \tag{37}$$

The general properties of solutions of (37) in the WKBJ limit have been studied in great detail by Wasow [34], and we shall repeatedly appeal to the results of that study. The differential operator D is restricted to be a polynomial in $-i\partial/\partial x$. Following Wasow [34], the system (37) is recast as a system of first-order equations

$$y_x = M[\omega_G, \mu(x)]\, y, \tag{38}$$

for a vector y of dimension n, M being a $n \times n$ matrix. Introducing, as before, the slow variable $X = \epsilon x$, (38) is written as

$$\epsilon y_X = M[X]y, \tag{39}$$

the dependence of M on ω_G remaining implicit.

The local spatial branches $k_j(X)$ at each location X are seen to be simply given by the eigenvalues $\lambda_j = ik_j$ of the matrix $M(X)$. As mentioned previously, only a single pair of eigenvalues, say (λ_1, λ_2), is assumed to experience branch switching in the complex X-plane. In such a situation, λ_1 and λ_2 pertain to left-moving waves at $X_r = -\infty$ and to right-moving waves at $X_r = +\infty$. Furthermore, the coefficients of $M(X)$ are taken to be holomorphic in some subdomain of the X-plane that includes the X_r-axis.

According to Wasow [34], the general equation (39) for the n-dimensional vector field y is then fully equivalent to a second-order system. Stokes lines are now defined by

$$\operatorname{Re}\left\{\frac{1}{\epsilon}\int_{X_0}^{X}\{\lambda_1(X)-\lambda_2(X)\}\,dX\right\}=0, \tag{40}$$

or equivalently by

$$\operatorname{Im}\left\{\frac{1}{\epsilon}\int_{X_0}^{X}\{k_1(X)-k_2(X)\}\,dX\right\}=0. \tag{41}$$

For Stokes lines emerging from a turning point X_s, one chooses $X_0=X_s$, and by definition one has $\lambda_1(X_s)=\lambda_2(X_s)$, or equivalently $k_1(X_s)=k_2(X_s)$. Stokes lines delineate subdomains D_j in the complex X-plane. In each sector D_j, independent solutions of (39) are asymptotic to a particular WKBJ approximation of wavenumber k_l, $l=1,2$. As a Stokes line is crossed, the solution may shift to another WKBJ approximation as expected from the Stokes phenomenon. The inner region surrounding the turning point determines the manner in which different WKBJ approximations need to be matched to obtain a global mode. It has been proven by Wasow [34] that the structure of a given turning point X_s only affects the WKBJ approximations associated with the colliding eigenvalues λ_1 and λ_2. In a sense, the spirit of the method very much evokes the center-manifold theory of nonlinear dynamical systems, as described for instance in Guckenheimer and Holmes [38]. The reader is referred to Wasow's work for details.

All the main results of Section 3.2 regarding second-order differential operators merely need to be transposed. Since crossing a Stokes line leads to a change from a dominant to a subdominant branch or vice versa, Lemma 1 holds: any deformed contour of the X_r-axis must cross at least two Stokes lines. Similarly, Lemma 2 still stands in a slightly altered form. If $\omega_{g,i}>\omega_{0,i\max}$, the quantity $(1/\epsilon)\operatorname{Im}\{k_1(X)-k_2(X)\}$ keeps the same sign along a straight line M parallel to the X_r-axis. Following the same arguments as in Section 3.2, $\operatorname{Im}\{(1/\epsilon)\int[k_1(X)-k_2(X)]dX\}$ increases or decreases monotonically as X travels along M, and only one Stokes line is crossed by M. In order to derive Theorem 1 and Corollary 1, we have to exclude pinching of the kind sketched in Figure 5. More specifically, when $\omega_{g,i}>\omega_{0,i\max}$, we must have

$$\min_{X\in M}\{\operatorname{Im}[k_2(X)-k_1(X)]\}>0. \tag{42}$$

Under these conditions, Corollary 1 remains valid: a system nowhere absolutely unstable ($\omega_{0,i\max}<0$) cannot sustain global modes with an $O(1)$ temporal growth rate $\omega_{g,i}>0$.

Turning our attention to the generalization of Theorem 2 and Corollary 2, we first need to find a straight horizontal path M in the complex X-plane such that the inequality (13), namely $\omega_{kk,i}<0$, is satisfied. The absolute frequency function $\omega_0(X)$ is then analytically continued into the complex X-plane as sketched

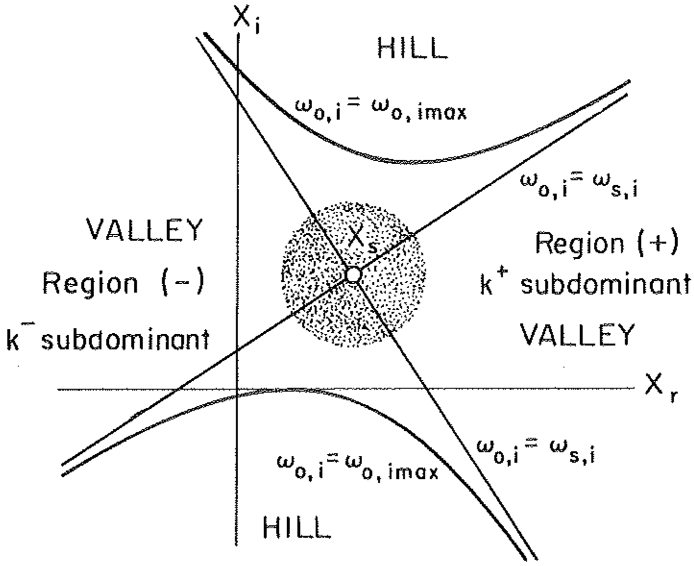

Figure 7. Sketch of $\omega_{0,i}$ = const curves in complex X-plane, in the vicinity of the saddle point X_s.

in Figure 7. As a straight horizontal line L is lowered in the complex ω-plane from $\omega_{g,i} = \omega_{0,i\max}$, the path M must be displaced to avoid pinching by L_1^{-1} and L_2^{-1} (Figure 4). On such a contour M, Lemma 2 is satisfied and application of Lemma 1 allows to rule out any global-mode frequency on L. This reasoning first fails when M is pinched by L_1^{-1} and L_2^{-1}, which takes place precisely as L reaches the frequency ω_s of the saddle point. Thus the temporal growth rate of the global mode is necessarily lower than $\omega_{s,i}$, as stated in Theorem 2 and Corollary 2. Finally, the arguments used in the proof of Theorem 3 only involve a local analysis around the turning point X_s. The structure of the inner region stays the same, independently of what may be the topology of the Stokes lines far away from X_s. The leading-order estimate of the global-mode frequency is therefore given by ω_s, as long as Assumptions 1 and 2 are valid.

Remarks: No general results are available when the dispersion relation involves transcendental functions and is therefore not expressible in terms of a polynomial of finite degree n. Nevertheless, it is very likely that the structure of the problem remains the same, and Theorems 1, 2, and 3 still apply. Extension of the above formulation to nonlinear systems is nontrivial. However, it is certainly possible to perform a weakly nonlinear analysis in the vicinity of the bifurcation to a global mode. This will be the object of future work. Preliminary results have been reported in [5].

4. Conclusions

The relationship between local and global instability properties has been firmly established in media that are slowly evolving in one spatial dimension X. Under very general conditions, we have shown (Theorem 1 and Corollary 1) that the leading-order approximation $\omega_{g,i}$ to the temporal growth rate of global modes is bounded from above by the maximum absolute growth rate $\omega_{0,i\,\max}$ over the domain. Consequently, a system nowhere absolutely unstable cannot sustain global modes with an $O(1)$ temporal growth rate. Under more restrictive conditions, i.e., the existence of a saddle point X_s of $\omega_0(X)$ in the complex X-plane where $(d\omega_0/dX)|_{X_s} = 0$ with $\omega_{0XX,i}(X_s) < 0$, we have obtained a much sharper upper bound $\omega_{s,i} \equiv \omega_{0,i}(X_s)$ for the global-mode growth rate (Theorem 2 and Corollary 2). Finally, it has been proven (Theorem 3) that this upper bound is actually reached: $\omega_{s,i}$ is indeed a leading-order estimate of the growth rate of the most unstable global mode.

Thus, given an explicit dispersion relation $\omega(k; X)$, the complex frequency of the dominant global mode is given, to leading-order in the WKBJ approximation, by

$$\omega_s = \omega_0(X_s), \tag{43}$$

where X_s is the closest saddle point of the absolute frequency $\omega_0(X)$ in the complex X-plane such that

$$\frac{d\omega_0}{dX}(X_s) = 0. \tag{44}$$

Equivalently, the dominant global mode frequency ω_g is given by

$$\omega_s = \omega(k_s; X_s), \tag{45}$$

where the complex pair (k_s, X_s) satisfies

$$\frac{\partial \omega}{\partial k}(k_s; X_s) = \frac{\partial \omega}{\partial X}(k_s; X_s) = 0. \tag{46}$$

Several spatially inhomogeneous unstable flows have previously been studied within the WKBJ framework. Examples include instabilities in the flow between concentric spheres [39], in Poiseuille flow within a curved pipe [40], and in Saffman-Taylor fingers [41]. In all these investigations the role of the absolute frequency $\omega_0(X)$ was not explicitly brought out: the presence of an additional reflection symmetry $x \to -x$ at the most unstable location led to the identity $\omega_{0,i\,\max} = \omega_{i,\max}^{\max}$, where $\omega_{i,\max}^{\max}$ is the maximum local temporal growth rate over all real X and over all real k. As a result the pocket of local instability near threshold in this class of flows coincides with the region of local absolute instability. Nonetheless, Theorems 2 and 3 and their corollaries remain valid, and they lead to the correct value of the most unstable global-mode frequency. A related "mode conversion" formulation has been developed by Fuchs et al. [42] to describe the evolution of instability waves in a weakly inhomogeneous plasma.

The criterion (43)–(46) has been applied to the determination of the preferred mode Strouhal number in two-dimensional jets by Monkewitz et al. [4].

The local instability properties of the measured mean velocity profiles along the jet axis were calculated to obtain an estimate of the saddle-point location X_s. The predicted Strouhal number was found to be 0.225, which should be compared with the experimental value 0.25.

The formalism that has been presented here is not restricted to systems in one space dimension. The cross-stream eigenfunctions can be incorporated in a systematic manner, starting from the fundamental equations of fluid motion linearized around a slowly diverging basic flow [28]. The turning-point structure remains the same, and one recovers the frequency selection criterion (35).

Appendix

An alternate derivation of Theorems 1 and 2 follows from integral considerations. Let us write the second-order system (20) in the form

$$\epsilon^2 \omega_{kk} \phi_{XX} + 2[\omega_G - \tilde{\omega}_0(X)]\phi = 0, \tag{A1}$$

and consider a subclass of systems where ω_{kk} is a complex constant independent of X. Since ϕ must vanish exponentially fast at infinity, the integral $\int_{-\infty}^{+\infty} \phi\bar{\phi}\, dX$ is bounded (an overbar denotes the complex conjugate). Multiplying (A1) by $\bar{\phi}$ and integrating over space, one obtains, after a single integration by parts,

$$\omega_G \int_{-\infty}^{+\infty} |\phi(X)|^2 \, dX = \int_{-\infty}^{+\infty} \tilde{\omega}_0(X) |\phi(X)|^2 \, dX + \frac{\epsilon^2 \omega_{kk}}{2} \int_{-\infty}^{+\infty} |\phi_X(X)|^2 \, dX. \tag{A2}$$

Taking the imaginary part of (A2) leads to

$$\omega_{G,i} \int_{-\infty}^{+\infty} |\phi(X)|^2 \, dX = \int_{-\infty}^{+\infty} \tilde{\omega}_{0,i}(X) |\phi(X)|^2 \, dX + \frac{\epsilon^2 \omega_{kk,i}}{2} \int_{-\infty}^{+\infty} |\phi_X(X)|^2 \, dX. \tag{A3}$$

The following inequality also holds:

$$\int_{-\infty}^{+\infty} \tilde{\omega}_{0,i}(X) |\phi(X)|^2 \, dX \le \tilde{\omega}_{0,i\,\max} \int_{-\infty}^{+\infty} |\phi(X)|^2 \, dX. \tag{A4}$$

Since, according to (13), $\omega_{kk,i} < 0$, we deduce from (A3) and (A4) that

$$\omega_{G,i} \int_{-\infty}^{+\infty} |\phi(X)|^2 \, dX \le \tilde{\omega}_{0,i\,\max} \int_{-\infty}^{+\infty} |\phi(X)|^2 \, dX, \tag{A5}$$

or

$$\omega_{G,i} \le \tilde{\omega}_{0,i\,\max}, \tag{A6}$$

which proves Theorem 1.

In order to prove Theorem 2, we simply need to extend (A1) to the complex X-plane. The function $\tilde{\omega}_0(X)$ is analytically continued, and the previous reasoning holds on a straight horizontal path M such that $X = X_i$, which is obtained by translating the X_r-axis in the vertical direction. The result (A6) then remains valid on M, with $\tilde{\omega}_{0,i\max}$ being the maximum of $\tilde{\omega}_{0,i}$ on M. In particular, if $\tilde{\omega}_0(X)$ admits a saddle point at $\tilde{X}_s$, one has

$$\omega_{G,i} \leq \tilde{\omega}_{s,i}, \tag{A7}$$

where $\tilde{\omega}_{s,i} = \omega_{0,i}(\tilde{X}_s)$. This proves Theorem 2.

Acknowledgments

We have benefited from many stimulating discussions with P. A. Monkewitz. This work was supported by the Air Force Office of Scientific Research under Grant F49620-85-C-0080.

References

1. J. M. Chomaz, P. Huerre, and L. G. Redekopp, Wave selection mechanisms in open flows, *Bull. Amer. Phys. Soc.* 31:1696 (1987).
2. J. M. Chomaz, P. Huerre, and L. G. Redekopp, Models of hydrodynamic resonances in separated shear flows, in *Proceedings of the Symposium on Turbulent Shear Flows*, 6th, Toulouse, 1987, pp. 3.2-1–6.
3. J. M. Chomaz, P. Huerre, and L. G. Redekopp, Bifurcation to local and global modes in spatially-developing flows, *Phys. Rev. Lett.* 60:25–28 (1988).
4. P. A. Monkewitz, P. Huerre, and J. M. Chomaz, Preferred modes in jets and global instabilities, *Bull. Amer. Phys. Soc.* 33:2273 (1988).
5. J. M. Chomaz, P. Huerre, and L. G. Redekopp, Effect of nonlinearity and forcing on global modes, in *Proceedings of the Conference on New Trends in Nonlinear Dynamical and Pattern-forming Phenomena* (P. Coullet and P. Huerre, Eds.), NATO ASI Series B: Physics, 237 (1990)
6. W. Koch, Local instability characteristics and frequency determination of self-excited wake flows, *J. Sound Vibration* 99:53–58 (1985).
7. R. T. Pierrehumbert, Local and global baroclinic instability of zonally varying flow, *J. Atmospheric Sci.* 41:2141–2162 (1984).
8. Y. Bar-Sever and L. O. Merkine, Local instabilities of weakly non-parallel large scale flows: WKB analysis, *Geophys. Astrophys. Fluid Dynamics* 41:233–286 (1988).
9. P. A. Sturrock, Amplifying and evanescent waves, convective and nonconvective instabilities, in *Plasma Physics* (J. E. Drummond, Ed.), McGraw-Hill, 1961, pp. 124–142.
10. R. J. Briggs, *Electron-Stream Interaction with Plasmas*, MIT Press, 1964.
11. E. M. Lifshitz and L. P. Pitaevskii, *Physical Kinetics*, Pergamon, 1981, Chapter 6.
12. A. Bers, Space-time evolution of plasma instabilities—absolute and convective, in *Handbook of Plasma Physics* (M. N. Rosenbluth and R. Z. Sagdeev, Eds.), North-Holland, 1983, pp. 1:451–1:517.
13. D. G. Crighton and P. Huerre, Model Problems for the Generation of Superdirective Acoustic fields by Wavepackets in Shear Layers, AIAA Paper 84-2295, 1984.
14. D. Rockwell and E. Naudascher, Self-sustained oscillations of impinging free-shear layers, *Annual Rev. Fluid Mech.* 11:67–94 (1979).
15. P. Huerre and P. A. Monkewitz, Absolute and convective instabilities in free shear layers, *J. Fluid Mech.* 159:151–168 (1985).
16. T. F. Balsa, Three-dimensional wavepackets and instability waves in free shear layers, *J. Fluid Mech.* 201:77–97 (1989).
17. M. Gaster, A theoretical model of a wavepacket in the boundary layer on a flat plate, *Proc. Roy. Soc. London Ser. A* 347:271–289 (1975).

18. C. M. Ho and P. Huerre, Perturbed free shear layers, *Annual Rev. Fluid Mech.* 16:365–424 (1984).
19. P. A. Monkewitz, The absolute and convective nature of instability in two-dimensional wakes at low Reynolds numbers, *Phys. Fluids* 31:999–1006 (1988).
20. G. S. Triantafyllou, M. S. Triantafyllou, and C. Chryssostomidis, On the formation of vortex street behind stationary cylinders, *J. Fluid Mech.* 170:461–477 (1986).
21. K. Hannemann and H. Oertel, Numerical simulation of the absolutely and convectively unstable wake, *J. Fluid Mech.* 199:55–88 (1989).
22. X. Yang and A. Zebib, Absolute and convective instability of a cylinder wake, *Phys. Fluids A* 1:689–696 (1989).
23. M. Provansal, C. Mathis and L. Boyer, Bénard–von Kármán instability: Transient and forced régimes, *J. Fluid Mech.* 182:1–22 (1987).
24. K. R. Sreenivasan, P. J. Strykowski, and D. J. Olinger, Hopf bifurcation, Landau equation and vortex shedding behind circular cylinders, in *Proceedings of the Forum on Unsteady Flow Separation* (K. N. Ghia, Ed), Vol. 52, ASME, 1987.
25. P. A. Monkewitz and K. D. Sohn, Absolute instability in hot jets, *AIAA J.* 26:911–916 (1988).
26. P. A. Monkewitz, D. W. Bechert, B. Barsikow, and B. Helman, Self-excited oscillations and mixing in a heated round jet, *J. Fluid Mech.* 213:611–639 (1990).
27. K. R. Sreenivasan, S. Raghu, and D. Kyle, Absolute instability in variable density round jets, *Exp. in Fluids* 7:309–317 (1989).
28. P. A. Monkewitz, P. Huerre, and J. M. Chomaz, Preferred modes in two-dimensional jets, in preparation.
29. P. Huerre, Spatio-temporal instabilities in closed and open flows, in *Instabilities and Nonequilibrium Structures* (E. Tirapegui and D. Villaroel, Eds.), Reidel, 1987, pp. 141–177.
30. P. A. Monkewitz, The role of absolute and convective instability in predicting the behavior of fluid systems, *European J. Mech. B/Fluids* 9:395–413 (1990).
31. P. Huerre and P. A. Monkewitz, Local and global instabilities in spatially-developing flows, *Annual Rev. Fluid Mech.* 22:473–537 (1990).
32. E. C. Titshmarsh, *Eigenfunction Expansions Associated with Second Order Differential Equations*, Parts I, II, Oxford U.P., 1946.
33. V. L. Pokrovskii and I. M. Khalatnikov, On the problem of above-barrier reflection of high energy particles, *Soviet Phys. JETP* 13:1207–1210 (1961).
34. W. Wasow, *Asymptotic Expansions for Ordinary Differential Equations*, Wiley, 1965.
35. E. Hille, *Lectures on Ordinary Differential Equations*, Addison-Wesley, 1969.
36. E. Hille, *Ordinary Differential Equations in the Complex Domain*, Wiley, 1976.
37. C. M. Bender and S. A. Orszag, *Advanced Mathematical Methods for Scientists and Engineers*, McGraw-Hill, 1978.
38. J. Guckenheimer and P. J. Holmes, *Nonlinear Oscillations, Dynamical Systems, and Bifurcations of Vector Fields*, Springer-Verlag, 1983.
39. A. M. Soward and C. A. Jones, The linear stability of the flow in the narrow gap between two concentric rotating spheres, *Quart. J. Mech. Appl. Math.* 36:19–42 (1983).
40. D. Papageorghiou, Stability of the unsteady viscous flow in a curved pipe, *J. Fluid Mech.* 182:209–233 (1987).
41. D. Bensimon, P. Pelcé, and B. I. Shraiman, Dynamics of curved fronts and pattern reflection, *J. Physique* 48:2081–2082 (1987).
42. V. Fuchs, K. Ko, and A. Bers, Theory of mode conversion in weakly inhomogeneous plasma, *Phys. Fluids* 24:1251–1261 (1981).

University of Southern California

(Received September 27, 1989)